

Microscopic approach to the structure of transition-metal glasses

Ch. Hausleitner and J. Hafner

Institut für Theoretische Physik, Technische Universität Wien, Wiedner Hauptstrasse 8-10, A-1040 Wien, Austria

(Received 31 May 1990)

A novel hybridized nearly-free-electron-tight-binding-bond approach to the interatomic forces in disordered transition-metal alloys is used to construct realistic models for the atomic structure of amorphous alloys.

The atomic structure of amorphous metallic alloys has been a subject of intense research for many years.^{1,2} Several distinct glass-forming alloy families have been established:³⁻⁵ (a) the transition-metal-semimetal (or "metalloid") systems (e.g., Fe-B or Ni-P), (b) the inter-transition-metal alloys (e.g., Ni-Zr or Fe-Ti), and (c) the simple-metal glasses (e.g., Mg-Zn or Ca-Al). Diffraction investigations and modeling studies have shown that the structure of metallic glasses of types (a) and (c) is rather well described as a polytetrahedral packing of atoms, modified by a certain degree of chemical short-range order and by the necessity to accommodate atoms of different size.⁵ For the transition-metal glasses of group (b), diffraction studies⁶⁻⁹ indicate a high degree of chemical as well as topological short-range order, leading to an atomic structure which is far more complex than that found in groups (a) or (c). Attempts to build structural models for the transition-metal glasses have been severely limited by the lack of reliable interatomic potentials.

Here we present a novel hybridized nearly-free-electron-tight-binding-bond (NFE-TBB) approach to the interatomic forces in disordered transition-metal alloys. These interatomic potentials are used to generate the first realistic models for the atomic structure of transition-metal glasses via a molecular-dynamics simulation. The analysis of these results establishes clear correlations between the short-range order in the liquid or amorphous alloy and the electronic structure.

The basic assumption is that the total energy E of a transition metal may be decomposed into contributions from the s and d electrons, $E = E_s + E_d$. The s -electron contribution is treated in a NFE approximation; i.e., we use pseudopotential perturbation theory¹⁰ to write E_s as the sum of a volume- and a pair-interaction term with a pair potential Φ_s . Within a TBB approximation the d -electron contribution to the total energy may be written in the form¹¹⁻¹³

$$E_d = \frac{1}{2} \sum_i \sum_{j (\neq i)} \Phi_{d,\text{rep}}(R_{ij}) + E_{d,\text{bond}}. \quad (1)$$

Assuming only one type of d orbital per site (i.e., assuming the d orbitals with different magnetic quantum numbers to be degenerate and neglecting the directionality of the d bond, which seems to be legitimate for liquid or glassy systems), E_{bond} is given by

$$E_{\text{bond}} = \sum_i \int_0^{E_F} (E - \varepsilon_{d,i}) n_i(E) dE. \quad (2)$$

That is, $E_{d,\text{bond}}$ measures the covalent bond energy resulting from the local density of states, $n_i(E)$, at the site i , calculated within a two-center orthogonal TB approximation. $\Phi_{d,\text{rep}}$ is a repulsive pair interaction provided by the electrostatic, exchange-correlation, and nonorthogonality contributions to the total energy.^{11,12} Hybridization between s and d states is taken into account by setting the numbers N_s and N_d of s and d electrons equal to the values resulting from a self-consistent band-structure calculation for the crystalline transition metal.

The local density of states may be calculated via a momentum expansion, and for the pure transition metals an approximation at the level of the second moment is found to be sufficient.^{13,14} In this case E_{bond} may be written as a sum over an attractive pairwise interaction $\Phi_{d,\text{bond}}(R_{ij})$ proportional to the average canonical d - d transfer integral $h(R_{ij}) = \{[(dd\sigma)^2 + 2(dd\pi)^2 + 2(dd\delta)^2]/5\}^{1/2} = \sqrt{14} \frac{2}{5} W_d(R_0/R_{ij})^5$. W_d is the width of the d band and R_0 the atomic radius. The transfer integral is adjusted to reproduce the correct width of the d band from a self-consistent calculation,¹⁵ and the pseudopotential core radius R_c is fitted to the zero-pressure equilibrium condition. These pair interactions yield a very accurate description of the structure of the molten transition metals.¹⁴

For a binary transition-metal alloy, the total energy will contain an additional contribution from the promotion energy^{12,16}

$$E_{d,\text{prom}} = C_A (N_{d,A} \varepsilon_{d,A} - N_{d,A}^0 \varepsilon_{d,A}^0) + C_B (N_{d,B} \varepsilon_{d,B} - N_{d,B}^0 \varepsilon_{d,B}^0), \quad (3)$$

where $\delta N_{d,I} = N_{d,I} - N_{d,I}^0$ and $\delta \varepsilon_{d,I} = \varepsilon_{d,I} - \varepsilon_{d,I}^0$, $I = A, B$, are the changes in the d -band occupancies $N_{d,I}$ and in the site energies $\varepsilon_{d,I}$ relative to their pure-metal reference values on alloying. The s -electron promotion energies are included in the pseudopotential approach. It may be shown that if $\delta N_{d,I}$ and $\delta \varepsilon_{d,I}$ are calculated self-consistently under the constraints

$$\delta N_{s,I} + \delta N_{d,I} = 0, \quad I = A, B \quad (4a)$$

(i.e., local charge neutrality, assuming that any change in the d -band occupancy is completely screened by the much more mobile s electrons) and

$$C_A \delta N_{d,A} + C_B \delta N_{d,B} = 0, \quad (4b)$$

the promotion energy is compensated to first order in

$\delta N_{d,I}$ by the intra-atomic d - d and s - d interactions, except for a site-diagonal term

$$E_{d,\text{prom}} + E_{\text{intra}} = C_A \delta N_{d,A} \varepsilon_A^0 + C_B \delta N_{d,B} \varepsilon_B^0, \quad (5)$$

which may be combined with the volume energy. This shows that the decomposition of the total energy into a volume term, an s -electron pair interaction Φ_s , and a d -electron pair interaction $\Phi_d = \Phi_{d,\text{rep}} + \Phi_{d,\text{bond}}$ is valid in a binary alloy. However, the second-moment approximation to $\Phi_{d,\text{bond}}$ is found to be inadequate in an alloy because it does not account for the form of the d band. Quite generally, the covalent bond energy may be written as^{11,16}

$$E_{d,\text{bond}} = \frac{1}{2} \sum_I \sum_{J (J \neq I)} h(R_{IJ}) \theta_{IJ}, \quad (6)$$

where θ_{IJ} is the bond order which is defined as the difference between the number of electrons in the bonding $2^{-1/2}(\varphi_I + \varphi_J)$ and in the antibonding states $2^{-1/2}(\varphi_I - \varphi_J)$ (the indices I and J stand for the atomic site as well as for the site occupancy). The bond order is obtained by integrating the off-diagonal Green's function $G_{IJ}(E)$ over the occupied states:^{11,16}

$$\theta_{IJ} = - \left[\frac{2}{\pi} \right] \int_0^{E_F} \text{Im} G_{IJ}(E) dE. \quad (7)$$

The calculation of the effective pair interactions for a transition-metal alloy proceeds as follows: (1) The pseudopotential and tight-binding parameters for the pure metals are determined as described above, and the values for Ni and Zr are given in Table I. (2) The electronic density of states (DOS) of the d band in the alloy is calculated for a reference configuration in a self-consistent Hartree-Fock TB approximation (using standard values¹⁷ for the intra-atomic and interatomic Coulomb integrals $u_{ss} = 0.5$ eV, $u_{sd} = 0.75$ eV, $u_{dd} = 1.6$ eV, and $V = 0.25$ eV), respecting the constraints of local charge neutrality (4a) and of constant number of d electrons (4b). The simplest reference lattice is a Bethe lattice^{18,19} (or Cayley tree) with coordination number 12. (3) Within the Bethe-lattice approximation, a closed set of equations may be constructed for the off-diagonal Green's functions $G_{IJ}(E)$.^{20,21} (4) The effective pair potentials are calculat-

ed for the self-consistent numbers ($N_{s,I}$ and $N_{d,I}$) of s and d electrons, site energies $\varepsilon_{d,I}$, and bond orders θ_{IJ} ($I, J = A, B$) resulting from (2) and (3); see Table I.

The electronic DOS of $\text{Ni}_{50}\text{Zr}_{50}$ calculated on the Bethe lattice shows a relatively narrow, nearly completely filled Ni d band overlapping with a broad Zr d band [Fig. 1(a)]. The position of the peak of the d band about 2 eV below the Fermi level agrees well with the results of soft-x-ray emission spectroscopy.²² From the imaginary part of the off diagonal Green's functions [Fig. 1(b)], we find that the Zr-Zr and Ni-Zr interactions are dominated by bonding combinations of nearest-neighbor d states, leading to large bond orders θ_{ZrZr} and θ_{NiZr} , whereas a nearly complete cancellation between bonding and antibonding interactions leads to a small θ_{NiNi} . This explains the pronounced nonadditivity of the pair interactions [Fig. 2(a)]. The individual contributions to the effective pair interactions are illustrated in Fig. 2(b) at the example of Φ_{NiZr} : around the nearest-neighbor distance the s -electron contribution is repulsive; the d -electron contribution is dominated by the bonding term and is strongly attractive.

The pair potentials have been used to construct a model for the glass via a molecular-dynamics (MD) algorithm. The simulation is started for the liquid alloy. After reaching equilibrium, the liquid (number density $n = 0.0524 \text{ \AA}^{-3}$) is compressed isothermally to the density of the glassy alloy ($n = 0.0584 \text{ \AA}^{-3}$) and reequilibrated (with the pair potentials recalculated for the density of the glass). Finally, the liquid is quenched to room temperature at constant volume. The simulations have been performed for ensembles of $N = 1372$ atoms in a periodically repeated box; the potentials have been cut at a distance of about 30% of the length of the edge of the MD cell. A fourth-order predictor-corrector algorithm with a time increment of $\delta t = 10^{-15}$ s was used for the integra-

TABLE I. Parameters of the interatomic potential for $\text{Ni}_{50}\text{Zr}_{50}$, with pure-metal references given in parentheses. See text for details.

	Ni	Zr	
R_c (Å)	0.58	1.22	
N_s	1.38 (1.40)	1.32 (1.30)	
N_d	9.62 (9.60)	4.68 (4.70)	
ε_d (Ry)	-0.362 (-0.363)	-0.185 (-0.184)	
W_d (Ry)	0.278	0.616	
R_c (Å)	1.377	1.771	
	Ni-Ni	Ni-Zr	Zr-Zr
θ_{IJ}	-0.654	-2.143	-2.113

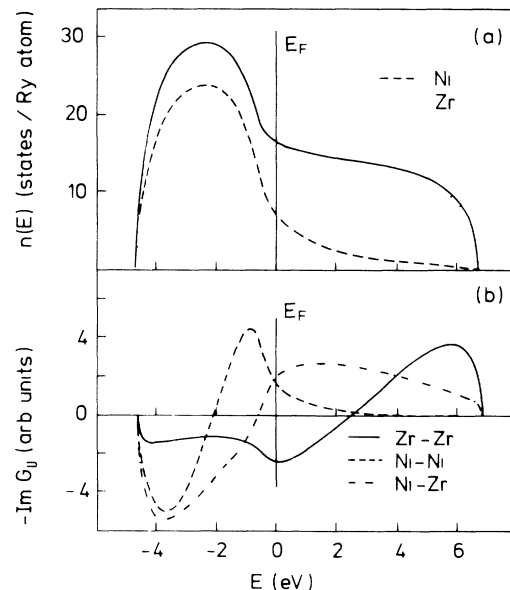


FIG. 1. (a) Electronic density of states $n(E)$ and (b) imaginary part of the off-diagonal Green's functions $G_{IJ}(E)$ for disordered $\text{Ni}_{50}\text{Zr}_{50}$.

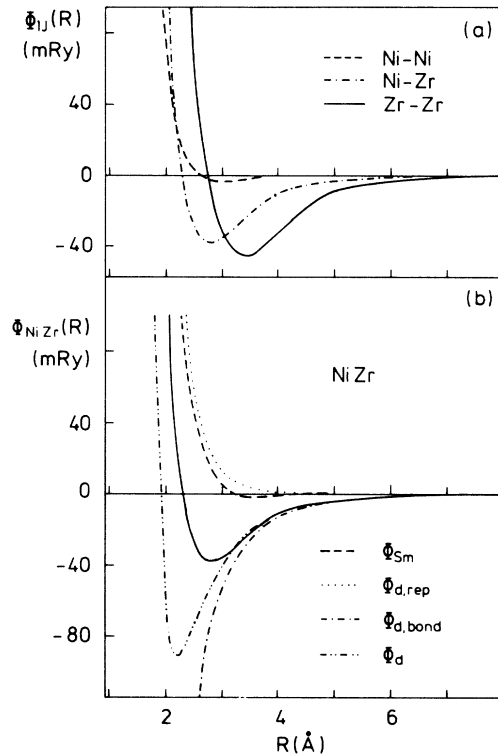


FIG. 2. (a) Effective interatomic potentials $\Phi_{IJ}(R)$ for $Ni_{50}Zr_{50}$. (b) Decomposition of $\Phi_{NiZr}(R)$ into s - and d -electron contributions (see text).

tion of the Newtonian equations of motion (for details, see Ref. 23). Typical runs allowed ~ 3000 steps for equilibration and ~ 2000 steps for production. The quenching rate was $dT/dt \approx 10^{14} \text{ K s}^{-1}$.

The resulting reduced pair-correlation functions $G_{IJ}(R) = 4\pi r n [g_{IJ}(R) - 1]$ for a $Ni_{50}Zr_{50}$ glass are shown in Fig. 3, together with the results of neutron-scattering experiments with isotropic substitution.⁹ We note (1) the good agreement between theory and experiment, which extends to almost every detail of the rather complex correlation functions, and (2) a pronounced chemical short-range order (CSRO) with partial coordination numbers which are very similar in the computer-generated

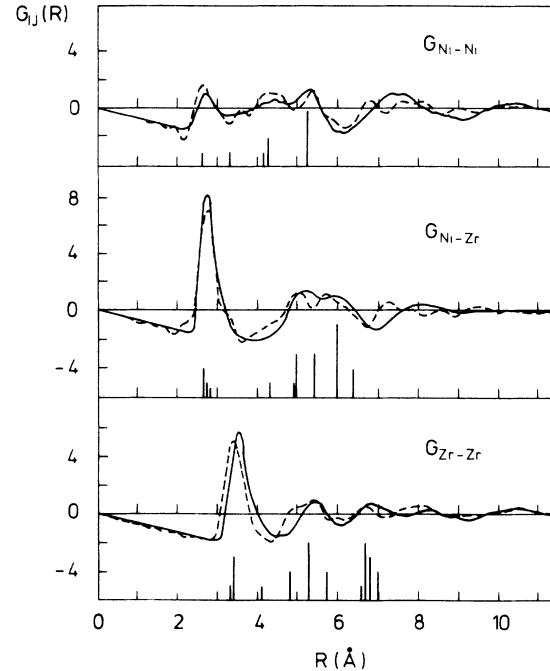


FIG. 3. Reduced pair correlation functions $G_{IJ}(R)$ for amorphous $Ni_{50}Zr_{50}$. Solid line, computer simulation; dashed line, neutron diffraction (Ref. 7). The vertical bars represent the interatomic distances in crystalline NiZr.

model and in the neutron-diffraction experiment, in the glassy and crystalline (CrB-type) phases²⁴ (see Table II). Both theory and experiment agree in that the tendency to form unlike-atom pairs around the Ni atoms is even larger in the glass than in the crystal. (3) The Ni-Zr interatomic distance in the glass is the same as in the crystal, and much smaller than the mean value of the Ni-Ni and Zr-Zr distances. Evidently this is a consequence of the strong covalent contribution to the Ni-Zr interaction. (4) The correspondence between the peaks in the G_{IJ} 's and the interatomic distances in the crystalline compound extends to the second and third coordination shells, suggesting a local and intermediate-range order in the glass which is closely related to the trigonal-prismatic structure of crystalline (CrB-type) NiZr.

TABLE II. Interatomic distances d_{IJ} and coordination numbers N_{IJ} .

	Theory		Experiment		NiZr crystal	
	d (Å)	N_{IJ}	d (Å)	N_{IJ}	d (Å)	N_{IJ}
Ni-Ni	2.68	2.2	2.63	3.3	2.62	2
					3.27	2
Ni-Zr	2.75	6.1	2.73	6.7	2.68	4
					2.73	2
					2.78	1
Zr-Zr	3.50	7.8	3.32	7.8	3.27	2
					3.43	2
					3.44	4

Similar calculations have been performed for all Ni- X glasses for which detailed information on the structure is available (X =Ti, V, Y, Zr, and Nb). The results show a clear correlation between the difference $\Delta N_d = N_{d,\text{Ni}} - N_{d,X}$ in the number of d electrons of the components and the degree of local order: a large ΔN_d leads to an electronic DOS close to the split-band limit, large differences in the bond-orders, and hence a strong SRO in Ni-Y, Ni-Ti, and Ni-Zr, a smaller ΔN_d leads to a common-band-type DOS, small differences in the bond orders, and a much weaker SRO in Ni-V and Ni-Nb.

In conclusion, we have developed a new interatomic

force field for disordered transition-metal alloys which we believe contains an important improvement: the dependence of the pair interaction on the bond order determined by the shape of the d band. We have shown that applications to simulations of glassy alloys are very promising. This will allow the study of the structure-property relationship of these materials at a level of detail not previously possible.

This work was supported by the Austrian Science Foundation under Project No. 7192.

-
- ¹D. Turnbull and M. H. Cohen, *J. Chem. Phys.* **34**, 120 (1961).
²N. E. Cusack, *The Physics of Structurally Disordered Materials* (Hilger, Bristol, 1987).
³J. Hafner, in *Glassy Metals I*, edited by H. J. Güntherodt and H. Beck (Springer, Berlin, 1981), p. 93.
⁴S. R. Elliot, *Physics of Amorphous Materials* (Longmans, London, 1983).
⁵D. R. Nelson and F. Spaepen, in *Solid State Physics*, edited by H. Ehrenreich and D. Turnbull (Academic, New York, 1989), Vol. 42, p. 1.
⁶T. Fukunaga, N. Watabe, and K. Suzuki, *J. Non-Cryst. Solids* **61&62**, 343 (1984).
⁷T. Fukunaga, N. Hayachi, N. Watanabe, and K. Suzuki, in *Rapidly Quenched Metals*, edited by S. Steeb and H. Warlimont (Elsevier, New York, 1985), p. 475.
⁸S. Lefebvre, A. Qivy, J. Bigot, Y. Calvayrac, and R. Bellissent, *J. Phys. F* **15**, L99 (1985).
⁹M. Maret, P. Chieux, P. Hicter, M. Atzmon, and W. L. Johnson, in *Rapidly Quenched Metals*, edited by S. Steeb and H. Warlimont (Elsevier, New York, 1985), p. 521.
¹⁰V. Heine, in *Solid State Physics*, edited by F. Seitz and D. Turnbull (Academic, New York, 1971), Vol. 24, p. 1.
¹¹A. P. Sutton, M. W. Finnis, D. G. Pettifor, and Y. Ohta, *J. Phys. C* **21**, 35 (1988).
¹²D. G. Pettifor and R. Podloucky, *J. Phys. C* **19**, 315 (1986).
¹³J. H. Wills and W. A. Harrison, *Phys. Rev. B* **28**, 4363 (1983).
¹⁴Ch. Hausleitner and J. Hafner, *J. Phys. F* **18**, 1025 (1988), and unpublished.
¹⁵V. L. Moruzzi, J. F. Janak, and A. R. Williams, *Calculated Electronic Properties of Metals* (Pergamon, New York, 1978).
¹⁶D. G. Pettifor, in *Many-Atom Interactions in Solids*, edited by R. Nieminen (Springer, Berlin, in press).
¹⁷D. Nguyen-Manh, D. Mayou, A. Pasturel, and F. Cyrot-Lackmann, *J. Phys. F* **15**, 1911 (1985).
¹⁸F. Brouers, Ch. Holzhey, and J. Franz, in *Excitations in Disordered Solids*, edited by M. F. Thorpe (Plenum, New York, 1982), p. 263.
¹⁹A. Pasturel and J. Hafner, *Phys. Rev. B* **34**, 8357 (1986).
²⁰Ch. Hausleitner and J. Hafner (unpublished).
²¹D. Nguyen-Manh, thesis, University of Grenoble, 1988 (unpublished).
²²J. M. Mariot, C. F. Hague, P. Oelhafen, and H. J. Güntherodt, *J. Phys. F* **16**, 1197 (1986).
²³A. Arnold, N. Mauser, and J. Hafner, *J. Phys. Condens. Matter* **1**, 1133 (1989).
²⁴P. Villars and L. D. Calvert, *Pearson's Handbook of Crystallographic Data for Intermetallic Phases* (American Society for Metals, Metals Park, OH 1985).